times more effective than any of the synthetic ligands and is $\sim 10^8$ times more effective than any of the hydroxamate siderophores.

The pM values of the sulfonated catecholates range from 24.9 from CYCAMS to 29.4 for MECAMS. The catecholates are clearly superior to the aminocarboxylate ligands such as DTPA (pM 24.7) and EDTA (pM 22.2). The pM values of the two most effective catecholates, LICAMS and MECAMS, are even higher than those of the hydroxamate siderophores. Other than enterobactin itself, the only ligands with sequestering ability equal to the sulfonated catecholates are the diphenolic ligands prepared and evaluated by Martell.[21,22] Of these, EHPG has shown some promise on the basis of in vivo iron removal studies,[23] even though its pM is a relatively modest 26.4.

A comparison of the pM values of the bidentate ligands tiron and DMBS with those of the tricatecholates clearly shows the importance of the possible number of coordination sites occupied by a ligand in determining its effectiveness at very dilute concentrations. The log β_3* for DMBS is 5.8, which is less than 1 log unit below the log K*'s of MECAMS and LICAMS and is actually higher than the log K*'s of TRIMCANS and CYCAMS. Its pM value, however, is a full 10 log units below MECAMS and LICAMS. This is an important consideration, since in vivo iron removal must of necessity entail low ligand concentrations.

Iron is stored in the body by two proteins, ferritin and hemosiderin. Both consist of a hydroxide–oxide–phosphate–iron(III) core surrounded by protein subunits,[24] and it is unlikely that simple chelating agents will remove significant amounts of this iron. However, transferrin, which is the plasma iron-transport protein, binds to specific receptor sights on ferritin and can readily mobilize this storage iron.[25] Thus the most likely mechanism for successful iron removal is to administer chelating agents which will remove the iron from transferrin and facilitate its excretion from the body and then allow the apotransferrin to mobilize the less accessible iron stores. Obviously the key factor in such an approach is finding a drug which will remove iron from transferrin. Transferrin has a pM value of only 23.6. From inspection of Table VI it is clear that almost all the catecholate ligands are capable thermodynamically of removing iron from transferrin. In the case of MECAMS, the competition equilibrium with transferrin favors the catecholate ligand by about 10^6, and even CYCAMS, which is the least effective of the sulfonated catecholates, is favored thermodynamically by a factor of 20. Thus it is obvious that the sulfonated catecholates represent a class of ligands which easily satisfy the thermodynamic requirements for a potential iron removal agent.

Since desferrioxamine B has a pM of 26.6, it also is thermodynamically capable of removing iron from transferrin. However, this exchange reaction is in fact too slow to be of clinical importance.[11] We have investigated the kinetics of iron removal from transferrin by several tricatecholate ligands and have found the reaction to proceed much more rapidly, with ~50% iron removal in 30 min. The details of this study have been reported separately.[11]

Summary

The sulfonated tricatecholates have been shown to combine a number of features which are necessary for an effective iron-sequestering agent. They are water soluble and are more resistant to air oxidation than their unsulfonated analogues. Unlike enterobactin, they are hydrolytically stable over a wide pH range. The lower ligand protonation constants of the sulfonated catecholates enhance their effectiveness at physiological pH. In particular, LICAMS and MECAMS are among the most effective iron ligands ever characterized. Finally, the catechols in general are capable of removing iron from transferrin at a reasonable rate under conditions where ferrioxamine B is almost totally ineffective. Animal tests of the in vivo efficacy of these compounds for iron decorporation are in progress, and the results will be reported separately.

Acknowledgment. We wish to thank Mary Kappel for her assistance in the least-squares analysis of the spectrophotometric data. This research is supported by the NIH through Grant HL 24775.

(21) L'Epllatenier, F.; Murase, I.; Martell, A. E. *J. Am. Chem. Soc.* **1967**, *89*, 837–843.
(22) Frost, A. E.; Freedman, H. H.; Westerback, S. J., Martell, A. E. *J. Am. Chem. Soc.* **1958**, *80*, 530–536.
(23) Pitts, C. G.; Gupta, G.; Estes, W. E.; Rosenkrantz, H.; Metterville, J. J.; Crumbliss, A. L.; Palmer, R. A.; Nordquest, K. W.; Hardy, K. A. S.; Whitcombe, D. R.; Byers, B. R.; Arceneaux, J. E. L.; Gaines, C. G.; Sciortino, C. V. *J. Pharmacol. Exp. Ther.* **1979**, *208*, 12–18.
(24) Ochiai, E. "Bioinorganic Chemistry"; Allyn and Bacon: Boston, 1977; p 171.
(25) Beck, W. S. "Hematology"; Massachusetts Institute of Technology, 1974; p 38.

Electron-Rich Carboranes. Studies of a Stereochemically Novel System, $(CH_3)_4C_4B_7H_9$, an 11-Vertex Arachno Cluster[1]

David C. Finster and Russell N. Grimes*

Contribution from the Department of Chemistry, University of Virginia, Charlottesville, Virginia 22901. *Received September 8, 1980*

Abstract: The controlled degradation of $(CH_3)_4C_4B_8H_8$ (I) in 95% ethanol in air gives $(CH_3)_4C_4B_7H_9$ (II). Electrophilic bromination of II produces 11-$Br(CH_3)_4C_4B_7H_8$ (III), which is shown in an X-ray diffraction study to have an open-cage structure with a bridging -$CH(CH_3)$- group across the open face; compounds II and III can be described as 11-vertex arachno cages. Deprotonation of II with NaH in THF generates the monoanion $(CH_3)_4C_4B_7H_8^-$ (IV) from which the CH proton on the bridging group has been removed. Protonation of IV gives a new isomer of $(CH_3)_4C_4B_7H_9$ (V), whose ^{11}B and ^1H FT NMR spectra indicate a substantially different cage geometry from that of II. The molecular structures of II–V and pathways for their interconversion are discussed in light of NMR, IR, mass spectroscopic, and X-ray evidence. Crystal data for III: $BrC_8B_7H_{20}$; mol wt 271.84; space group $P\bar{1}$; $Z = 2$; $a = 7.764$ (3), $b = 8.352$ (5), $c = 12.317$ (6) Å; $\alpha = 94.53$ (5), $\beta = 95.41$ (5), $\gamma = 120.51$ (5)°; $V = 678$ Å^3; $R = 0.057$ for 1404 independent reflections having $F_o^2 > 3\sigma(F_o^2)$.

The high-yield preparation[2] of the tetracarbon carborane $(CH_3)_4C_4B_8H_8$ (I) has opened up new, intriguing avenues in boron cage synthesis, and a variety of 11- to 14-vertex metallacarboranes has been obtained[3] by insertion of transition metals into I, both

0002-7863/81/1503-2675$01.25/0

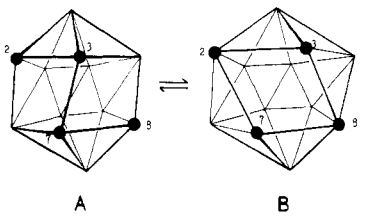

Figure 1. Equilibrium[7] between $(CH_3)_4C_4B_8H_8$ isomers A (established) and B (proposed). Solid circles represent C–CH_3 groups; other vertices are BH.

directly and via the carborane dianion $(CH_3)_4C_4B_8H_8^{2-}$. Compound I is an "electron-rich"[4] nido cage, with 28 skeletal bonding electrons compared to the requirement[5] of 26 for a closo (icosahedral) 12-vertex polyhedron, and consequently adopts a distorted cage geometry; moreover, many of the metallacarboranes derived from I also have unusual, often unique, cage structures.[3,6] Most of our attention has been directed to the structural consequences of metal insertion into I. However, a recent study[7] did examine the introduction of additional electrons to I, forming the 12-vertex, 30-electron $(CH_3)_4C_4B_8H_8^{2-}$ dianion which has a more open (arachno) structure than I itself.

Clearly other aspects of the chemistry of I merit attention as well, and in parallel with the properties of the well-known icosahedral $C_2B_{10}H_{12}$ carboranes,[8] it was of interest to explore the degradation of I to smaller cage systems. The present investigation was concerned with the conversion of I to a C_4B_7 species and the quite unexpected stereochemistry which was uncovered in the course of events.

Results and Discussion

Cage Degradation of $(CH_3)_4C_4B_8H_8$. The carborane $(CH_3)_4C_4B_8H_8$ (I) is a white, air-stable solid, mp 138 °C, which is remarkably volatile at room temperature (in contrast to the $C_2B_{10}H_{12}$ carboranes, which are essentially nonvolatile).[2] The distorted-icosahedral solid-state structure of I (Figure 1, isomer A) was determined crystallographically several years ago,[9] and recently the cage structural parameters were more precisely established from an X-ray study of the *B*(4)-ferrocenyl derivative which was shown to have the same framework geometry.[10] In solution, isomer A exists in equilibrium with a second isomer (B, Figure 1) which has not been isolated; on removal of solvent the mixture reverts entirely to A. The geometry depicted for B has been proposed[7] from ^{11}B and ^1H FT NMR observations and by consideration of the known structures of metal complexes derived from I and its dianion. This behavior is very different from that of 1,2-$C_2B_{10}H_{12}$, which is nonfluxional in solution and isomerizes only above 400 °C, and then irreversibly.[8]

In light of the well-known degradation of 1,2-$C_2B_{10}H_{12}$ to $C_2B_9H_{12}^-$ by the action of Lewis bases,[11a,b] similar behavior was expected for I. Compound I does not react with $(C_2H_5)_3N$ or tetrahydrofuran (THF) in the absence of air, but it does undergo slow, controlled degradation over several hours in 95% ethanol at room temperature in air, forming a new carborane, $(CH_3)_4$-

Table I. 32.1-MHz ^{11}B FT NMR Data[a]

compd	δ[b] (J_6 Hz)	rel area
$(CH_3)_4C_4B_7H_9$ (II)	8.7 (128)	1
	2.9 (181)	2
	−3.3 (156)	1
	−7.3 (150)	1
	−11.1 (180)	1
	−41.7 (156)	1
$(CH_3)_4C_4B_7H_8Br$ (III)	8.4 (156)	1
	0.5 (166)	2
	−2.2 (150)	1
	−7.3	1
	−8.6 (182)	1
	−41.7 (156)	1
$Na^+(CH_3)_4C_4B_7H_8^-$ (IV)[c]	7.6 (116)	1
	2.7 (132)	1
	−4.3 (147)	2
	−17.1 (122)	1
	−26.8 (146)	2
$(CH_3)_4C_4B_7H_9$ (V), second isomer	4.4 (147)	3
	−7.8 (*d*)	1
	−10.5 (*d*)	1
	−12.0 (*d*)	1
	−40.3 (156)	1

[a] Spectra obtained in $CDCl_3$, except where otherwise noted. [b] $BF_3{\cdot}O(C_2H_5)_2$ shift is 0, positive shifts downfield. [c] Spectrum obtained in CD_3CN. [d] J_{BH} coupling obscured by peak overlap.

Table II. 100-MHz ^1H NMR Data

compd (solvent)	δ[a] CH_3 (area 3)	$CH_3(7)$[b] (area 3)	H(7) (area 1)	BHB (area 1)	BH (area)
II ($CDCl_3$)	2.02	1.08	2.04	−1.65[c]	3.7 (1)
	1.95				2.9 (1)
	1.30				2.5 (1)
					2.4 (2)
					1.3 (1)
					0.4 (1)
II (C_6D_6)	1.81	0.87	1.8	−1.57[c]	3.8 (1)
	1.39				3.5 (1)
	0.89				3.0 (3)
					2.5 (1)
					1.6 (1)
III ($CDCl_3$)	2.01	1.09	2.3	−1.3[c]	3.7 (1)
	1.95				3.6 (1)
	1.33				3.1 (1)
					2.9 (1)
					2.6 (1)
					1.6 (1)
					0.4 (1)
IV (CD_3CN)	1.98			−1.53[d]	*e*
	1.55				
	1.05				
	0.99				
V ($CDCl_3$)	1.97	1.22	2.45	*f*	*e*
	1.90				
	1.15				
V (C_6D_6)	1.73	0.97	2.2	−1.65[c]	*e*
	1.29				
	0.71				

[a] Chemical shifts referenced to $(CH_3)_4Si$. [b] Doublet due to coupling to CH(7), $J_{HH} \simeq 6$ Hz. [c] Doublet of doublets, apparent 1:2:1 triplet, $J_{HH} = 10$ Hz. [d] Apparent 1:3:3:1 quartet (?), $J_{HH} = 10$ Hz. [e] BH protons not readily distinguished. [f] Spectrum obtained without ^{11}B decoupling; bridge hydrogens not observed.

(1) Based in part on: Finster, D. C. Ph.D. Dissertation, University of Virginia, 1980.

(2) Maxwell, W. M.; Miller, V. R.; Grimes, R. N. *Inorg. Chem.* **1976**, *15*, 1343.

(3) Grimes, R. N.; Sinn, E.; Pipal, J. R. *Inorg. Chem.* **1980**, *19*, 2087 and references therein.

(4) This term is used in a relative descriptive sense to indicate the presence of excess skeletal electrons beyond the $2n + 2$ normally required to fill the $n + 1$ bonding molecular orbitals in a closo *n*-vertex polyhedron.[5]

(5) (a) Wade, K. *Adv. Inorg. Chem. Radiochem.* **1976**, *18*, 1. (b) Mingos, D. M. P. *Nature (London), Phys. Sci.* **1972**, *236*, 99. (c) Rudolph, R. W. *Acc. Chem. Res.* **1976**, *9*, 446.

(6) Grimes, R. N. *Acc. Chem. Res.* **1978**, *11*, 420.

(7) Grimes, R. N.; Pipal, J. R.; Sinn, E. *J. Am. Chem. Soc.* **1979**, *101*, 4172.

(8) Beall, H. In "Boron Hydride Chemistry"; Muetterties, E. L., Ed.; Academic Press: New York, 1975.

(9) Freyberg, D. P.; Weiss, R.; Sinn, E.; Grimes, R. N. *Inorg. Chem.* **1977**, *16*, 1847.

(10) Grimes, R. N.; Maxwell, W. M.; Maynard, R. B.; Sinn, E. *Inorg. Chem.* **1980**, *19*, 2981.

(11) (a) Wiesboeck, R. A.; Hawthorne, M. F. *J. Am. Chem. Soc.* **1964**, *86*, 1642. (b) Zakharkin, L. I.; Kalinin, V. N. *Dokl. Akad. Nauk SSSR* **1965**, *163*, 110. (c) Tebbe, F. N.; Garrett, P. M.; Hawthorne, M. F. *J. Am. Chem. Soc.* **1968**, *90*, 869.

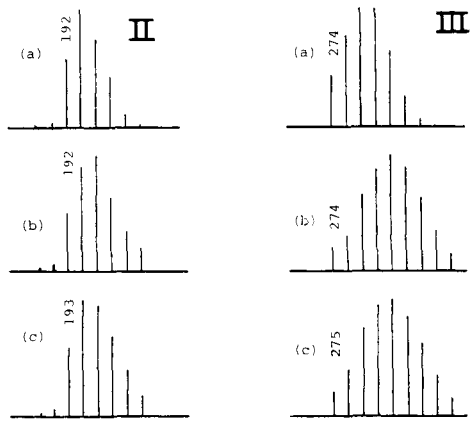

Figure 2. Mass spectroscopic parent group intensities for II $[(CH_3)_4C_4B_7H_9]$ and III $[(CH_3)_4C_4B_7H_8Br]$, with horizontal scales in units of m/e. II: (a), calculated for $(CH_3)_4C_4B_7H_7$; (b), electron-impact (EI) spectrum of II; (c), chemical ionization (CI) spectrum in CH_4. III: (a), calculated for $(CH_3)_4C_4B_7H_8Br$; (b), EI spectrum; (c), CI spectrum in CH_4. CI spectra exhibit cutoffs one mass unit higher than EI spectra due to protonation by methane. For both compounds, CI spectra in Ar/H_2O are similar to the spectra in CH_4 except for the appearance of M + 17 peaks arising from hydration.

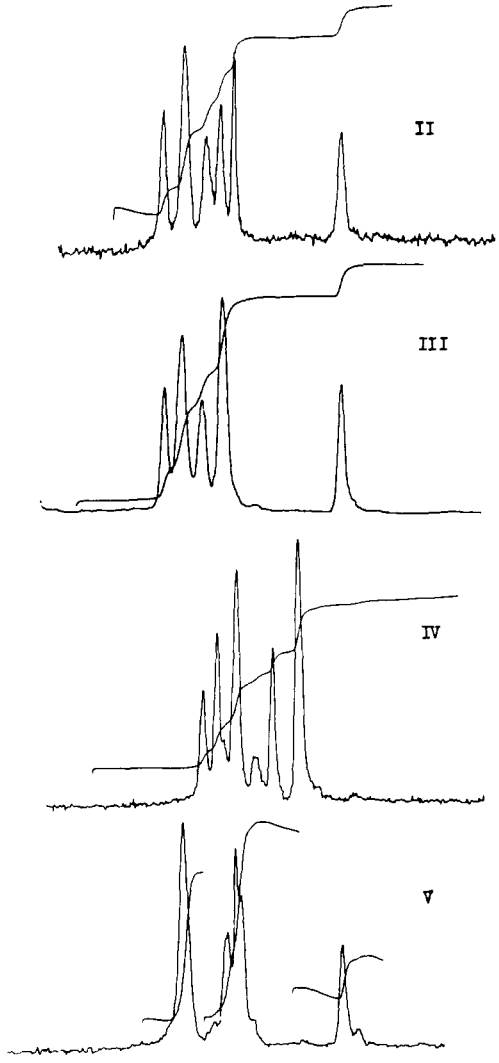

Figure 3. 32.1-MHz proton-decoupled ^{11}B FT NMR spectra of II, III, and V (all in $CDCl_3$ solution) and IV (CD_3CN). Chemical shifts and coupling constants are given in Table I.

$C_4B_7H_9$ (II). Compound II, a white, air-stable solid, mp 190 °C dec, has been isolated in 40%–60% yields. The presence of water is evidently essential in this reaction, since I is unreactive toward

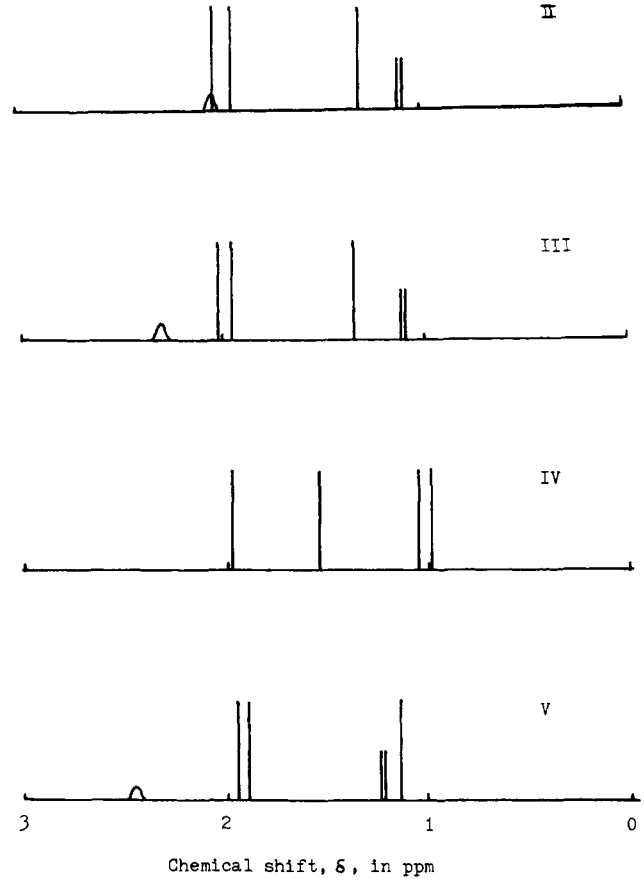

Figure 4. Simplified representations of the H–C ^1H FT NMR resonances of II–V. The H–C_{bridge} signals are shown as small broad peaks, the methyl singlets as tall lines, and the methyl doublets as shorter lines.

dry ethanol or methanol; in 95% aqueous THF in air, I decomposes to uncharacterizable products, as is also the case when I is treated with $(C_2H_5)_3N$ in air.

The degradation of I can be written as

$$(CH_3)_4C_4B_8H_8 + 3H_2O \rightarrow (CH_3)_4C_4B_7H_9 + B(OH)_3 + H_2$$

which is analogous to the conversion of $C_2B_9H_{11}$ to $C_2B_7H_{13}$,[11c] but the actual stoichiometry may be more complex than the equation suggests. Carborane II is identical with a product, previously unreported, which was obtained[12] in low yield in the reaction of $Na^+[(CH_3)_2C_2B_4H_5]^-$ with $FeCl_2$ *at room temperature* (see Experimental Section).

Structural Characterization of II. Compound II was initially formulated as $(CH_3)_4C_4B_7H_7$ on the basis of its chemical ionization (CI) and electron impact (EI) mass spectra, which exhibit sharp cutoffs at m/e 193 (M + 1) and 192, respectively (Figure 2). Other than small peaks attributable to ^{13}C-containing ions, there are no significant EI intensities above m/e 192, implying the absence of "extra" (e.g., B–H–B bridging) hydrogen atoms. Nonetheless, subsequent work established that two extra hydrogens are indeed present, and II is in fact $(CH_3)_4C_4B_7H_9$ (mol wt 194). This conclusion was derived from FT NMR and IR spectra of II and its B-bromo derivative (III) (Figures 3 and 4; Tables I–III), the mass spectrum of III (Figure 2), and an X-ray crystal structure determination on III, described below. Hence the low intensities of m/e 193 and 194 peaks in the mass spectra of II are attributed to extremely facile loss of two hydrogen atoms in the heated sources of the spectrometers, such that only the spectra of $(CH_3)_4C_4B_7H_7$ are observed. In the bromo derivative, the loss of hydrogen is not complete and the expected parent peaks are, in fact, present.

Bromination of II. Treatment of II with Br_2 in carbon disulfide solution over $AlCl_3$ produced a monobromo derivative, $(CH_3)_4$-

(12) Weiss, R.; Grimes, R. N., unpublished results.

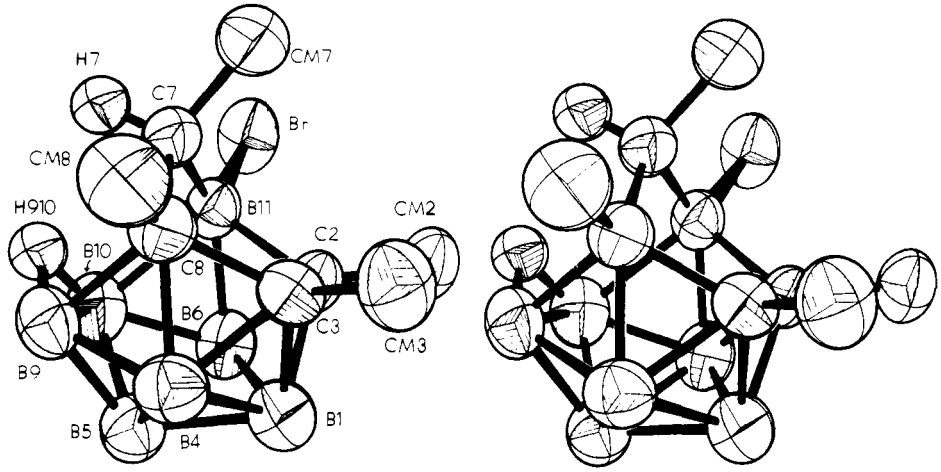

Figure 5. Stereoview of the molecular structure of III [11-Br$(CH_3)_4C_4B_7H_8$], with nonhydrogen atoms shown as 50% thermal ellipsoids. Hydrogens other than H(7) and H(910) are omitted for clarity. H(7) and H(910) are depicted as spheres of arbitrary radius.

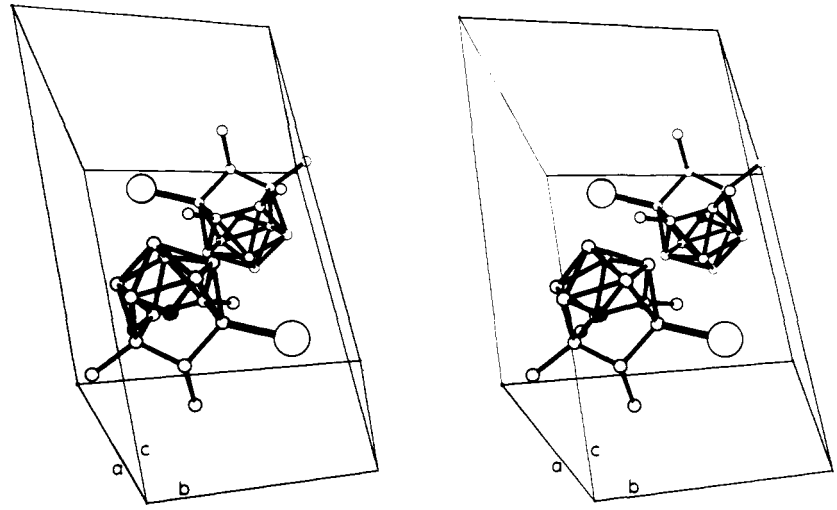

Figure 6. Unit cell packing of III.

Table III. IR Data[a] (cm^{-1}, KBr pellet)

$(CH_3)_4C_4B_7H_9$ (II)

2960 s, 2930 s, 2880 s, 2600 sh, 2560 s, 2480 s, 1950 w br, 1620 w br, 1565 w br, 1440 s, 1395 m, 1385 s, 1365 s, 1340 w, 1250 m, 1220 w, 1150 m, 1100 m, 1080 m, 1025 s, 1005 m, 980 s, 910 s, 800 s, 780 s, 720, 700 m, 680 w

11-Br$(CH_3)_4C_4B_7H_8$ (III)

2960 s, 2920 s, 2860 s, 2570 s br, 1950 w br, 1725 w br, 1560 w br, 1440 s, 1395 m, 1385 s, 1365 s, 1340 m, 1260 s, 1230 m, 1195 m, 1155 m, 1070 s br, 1020 s br, 1000 sh, 990 m, 980 m, 935 m, 910 m, 880 sh, 855 s, 795 s br, 725 m, 700 w, 695 w, 660 w, 625 m

$(CH_3)_4C_4B_7H_9$, Second Isomer (V)

2960 s, 2930 s, 2870 m, 2830 m, 2590 s br, 2480 s, 1975 w br, 1530 w br, 1550 w br, 1460 sh, 1450 s, 1380 s, 1320 w, 1250 w, 1230 w, 1160 w, 1120 w, 1070 s, 1040 w, 1005 s, 985 s, 910 s, 810 s, 780 w, 760 w, 720 s, 700 m, 665 w, 640 w

[a] Key: s = strong, m = medium, w = weak, br = broad, sh = shoulder.

$C_4B_7H_8Br$ (III), which was isolated in 50% yield as a colorless, air-stable solid (mp 225 °C). From the close similarity of the ^{11}B and ^1H FT NMR spectra of II and III (Figures 3 and 4), it is apparent that these species have the same cage geometry and that III is in fact a bromo-substituted derivative of II (see discussion below). The cage structure of III was subsequently established from an X-ray study of III as follows.

***Crystal Structure of* 11-Br$(CH_3)_4C_4B_7H_8$ (III).** The molecular geometry is illustrated in Figures 5 and 6, with relevant data listed in Tables IV–VII. The cage framework consists of an open C_3B_7 basket with a "handle" formed by a bridging -$CH(CH_3)$- group across the opening. The three skeletal carbon atoms occupy vertices on the open rim, and all four nonmethyl carbons retain a contiguous relationship. The bromine atom is attached to B(11), adjacent to the bridging carbon [C(7)], and the two "extra" hydrogens are located on C(7) and in a B–H–B bridge as shown. There are no unusual B–B or B–C bond distances (Table V) but the two framework C–C bonds [C(2)–C(3) and C(3)–C(8)] are relatively long for interactions between *low-coordinate* skeletal carbon atoms.[13] The bridging hydrogen, H(910) is only 1.99 Å from the methylenic hydrogen, H(7), or 0.4 Å less than the typical van der Waals H–H separation; as a consequence of this crowding, the B–H–B bridge is unsymmetrical and skewed toward B(10).

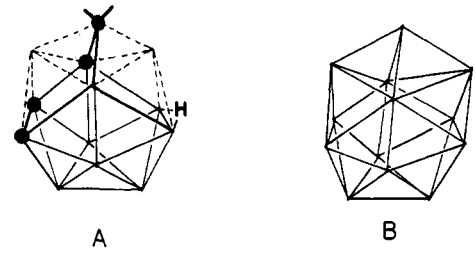

Figure 7. (A) Cage geometry of III depicted as an arachno fragment of a 13-vertex closo polyhedron (B).

The C_4B_7 cage geometry in III (and II) can usefully be described in several ways. The molecule may be viewed as a 13-

(13) Pipal, J. R.; Grimes, R. N. *Inorg. Chem.* **1978**, *17*, 10.

Table IV. Positional and Thermal Parameters and Their Estimated Standard Deviations for 11-Br$(CH_3)_4C_4B_7H_8$ (III)[a]

atom	x	y	z	U_{11}	U_{22}	U_{33}	U_{12}	U_{13}	U_{23}
Br	0.0661 (1)	0.23958 (8)	0.09389 (7)	0.1073 (4)	0.0586 (2)	0.0885 (5)	0.0496 (2)	−0.0162 (4)	−0.0123 (3)
C(2)	0.4332 (8)	0.7658 (7)	0.3153 (5)	0.050 (3)	0.048 (2)	0.058 (4)	0.024 (2)	0.012 (3)	0.007 (2)
C(3)	0.3115 (8)	0.5529 (6)	0.2999 (5)	0.054 (3)	0.043 (2)	0.052 (3)	0.026 (2)	0.005 (3)	0.012 (2)
C(7)	0.2838 (8)	0.6729 (7)	0.1214 (5)	0.070 (3)	0.061 (2)	0.048 (4)	0.043 (2)	0.007 (3)	0.007 (2)
C(8)	0.3508 (8)	0.8357 (7)	0.2158 (5)	0.062 (3)	0.045 (2)	0.059 (4)	0.028 (2)	0.017 (3)	0.015 (2)
C(M2)	0.6571 (9)	0.8760 (9)	0.3601 (6)	0.056 (3)	0.075 (3)	0.087 (5)	0.028 (2)	0.000 (3)	0.004 (3)
C(M3)	0.4132 (9)	0.4444 (8)	0.3300 (6)	0.085 (3)	0.070 (3)	0.072 (4)	0.048 (2)	−0.002 (3)	0.010 (3)
C(M7)	0.4647 (10)	0.6810 (8)	0.0787 (6)	0.094 (3)	0.088 (3)	0.069 (4)	0.060 (2)	0.017 (3)	0.011 (3)
C(M8)	0.4948 (10)	1.0335 (8)	0.1910 (6)	0.079 (3)	0.055 (3)	0.105 (5)	0.029 (2)	0.035 (4)	0.032 (3)
B(1)	0.263 (1)	0.6589 (9)	0.4055 (7)	0.060 (3)	0.051 (3)	0.068 (5)	0.027 (2)	0.009 (4)	0.005 (3)
B(4)	0.069 (1)	0.4701 (8)	0.3084 (7)	0.059 (3)	0.045 (3)	0.071 (5)	0.023 (2)	0.006 (4)	0.014 (3)
B(5)	0.045 (1)	0.6684 (9)	0.3519 (7)	0.065 (4)	0.061 (3)	0.063 (5)	0.035 (2)	0.008 (4)	0.008 (3)
B(6)	0.292 (1)	0.8577 (9)	0.3481 (6)	0.067 (4)	0.052 (3)	0.059 (5)	0.030 (2)	0.011 (3)	0.005 (3)
B(9)	0.099 (1)	0.7929 (8)	0.2367 (7)	0.067 (3)	0.050 (3)	0.073 (5)	0.037 (2)	0.012 (3)	0.012 (3)
B(10)	−0.053 (1)	0.5388 (9)	0.2176 (7)	0.054 (3)	0.059 (3)	0.082 (5)	0.028 (2)	0.011 (4)	0.018 (3)
B(11)	0.153 (1)	0.4889 (8)	0.1787 (6)	0.065 (3)	0.045 (3)	0.054 (4)	0.033 (2)	0.002 (3)	0.003 (3)

atom[b]	x	y	z	B, Å^2	atom[b]	x	y	z	B, Å^2
H(21)	0.727 (8)	1.015 (7)	0.385 (5)	6 (1)	H(81)	0.616 (7)	1.043 (6)	0.172 (4)	4 (1)
H(22)	0.671 (7)	0.834 (7)	0.423 (5)	5 (1)	H(82)	0.554 (8)	1.143 (7)	0.257 (5)	5 (1)
H(23)	0.725 (8)	0.868 (7)	0.305 (5)	6 (2)	H(83)	0.428 (8)	1.062 (7)	0.138 (5)	6 (1)
H(31)	0.312 (8)	0.329 (7)	0.334 (5)	6 (1)	H(4)	−0.014 (7)	0.330 (6)	0.336 (4)	4 (1)
H(32)	0.503 (8)	0.501 (7)	0.405 (5)	7 (2)	H(5)	−0.037 (7)	0.688 (7)	0.424 (4)	4 (1)
H(33)	0.463 (9)	0.433 (8)	0.266 (5)	7 (2)	H(6)	0.377 (7)	0.995 (6)	0.404 (4)	4 (1)
H(71)	0.542 (7)	0.647 (7)	0.126 (5)	5 (1)	H(7)	0.204 (7)	0.678 (6)	0.060 (4)	4 (1)
H(72)	0.558 (8)	0.811 (8)	0.051 (5)	6 (2)	H(9)	0.051 (7)	0.895 (6)	0.220 (4)	4 (1)
H(73)	0.405 (6)	0.590 (6)	0.019 (4)	3 (1)	H(910)	0.001 (7)	0.657 (6)	0.154 (4)	4 (1)
					H(10)	−0.195 (8)	0.481 (7)	0.193 (5)	6 (2)

[a] The form of the anisotropic thermal parameter is $\exp[-2\pi^2(U_{11}h^2a^{*2} + U_{22}k^2b^{*2} + U_{33}l^2c^{*2} + 2U_{12}hka^*b^* + 2U_{13}hla^*c^* + 2U_{23}klb^*c^*)]$. [b] For hydrogen atoms standard isotropic B values are given.

Table V. Bond Lengths (Å) in 11-Br$(CH_3)_4C_4B_7H_8$ (III)

B(1)-C(2)	1.692 (6)	B(5)-B(10)	1.768 (7)
B(1)-C(3)	1.735 (6)	B(6)-B(10)	1.712 (6)
B(1)-B(4)	1.773 (6)	B(6)-B(11)	1.770 (7)
B(1)-B(5)	1.804 (7)	C(7)-C(8)	1.546 (5)
B(1)-B(6)	1.771 (6)	C(7)-B(11)	1.616 (6)
C(2)-C(3)	1.516 (4)	C(7)-C(M7)	1.517 (5)
C(2)-B(6)	1.660 (6)	C(7)-H(7)	0.952 (3)
C(2)-B(11)	1.698 (5)	C(8)-B(9)	1.846 (6)
C(2)-C(M2)	1.519 (5)	C(8)-C(M8)	1.531 (5)
C(3)-B(4)	1.685 (6)	B(9)-B(10)	1.811 (6)
C(3)-C(8)	1.611 (5)	B(9)-H(910)	1.301 (4)
C(3)-C(M3)	1.512 (5)	B(10)-B(11)	1.937 (6)
B(4)-B(5)	1.771 (7)	B(10)-H(910)	1.236 (6)
B(4)-C(8)	1.752 (6)	B(11)-Br	1.994 (4)
B(4)-B(9)	1.758 (7)	⟨B-$H_{terminal}$⟩	1.097
B(5)-B(6)	1.806 (6)	⟨C-H_{Me}⟩	0.957
B(5)-B(9)	1.781 (6)		
	Nonbonded Distances (Å)		
C(7)-C(2)	2.52	C(7)-B(10)	2.70
C(7)-C(3)	2.43	H(7)-H(910)	1.99
C(7)-B(9)	2.59		

vertex closo polyhedron[14] from which two nonadjacent vertices have been removed (Figure 7), which precisely fits the definition of an arachno cage as a closo system with two missing vertices.[17] Compounds II and III are the first known 11-vertex carboranes with this geometry, although *arachno*-$[(C_6H_5)_3P]_2MC_2B_8H_{11}$ (M = Cu, Ag, Au) complexes are known.[16] Since II and III contain 28 skeletal electrons in an 11-vertex framework (on the basis of contributions of three from each C–CH_3 unit, two from each BH, and one from each "extra" hydrogen), they are $(2n + 6)$-electron systems in conformity[5] with the observed arachno geometry. If one compares II with the 11-vertex closo system $C_2B_9H_{11}$, a 24-electron $(2n + 2)$ cage, the introduction of four skeletal electrons (as in II) is seen to produce cage opening via lengthening of the four interactions between the apex atom [C(7)] and vertices 2, 3, 9, and 10.

Alternatively, one may regard the $CH(CH_3)$ bridge as "outside" the cage and linked via two localized electron-pair bonds to the remaining $(CH_3)_3C_3B_7H_8$ moiety, which is itself isoelectronic and isostructural with $B_{10}H_{14}$. In this sense, II and III would qualify as the first three-carbon analogues of $B_{10}H_{14}$.

NMR Spectra of II and III. As noted above, the ^{11}B and ^1H FT NMR spectra of the two species are closely similar, and they are entirely consistent with the crystallographically determined structure. The resonance at δ −7.3 in III is assigned to B(11)–Br since no coupling to a terminal proton is observed; there is no indication in either spectrum of the presence of more than one isomer.

The ^1H spectra (Figure 4) exhibit four nonequivalent methyl resonances, one of which is split into a doublet; this clearly arises from coupling of the methyl protons on C(M7) to the proton H(7). From the fact that C(2) and C(3) occupy similar coordination sites, the closely spaced low-field methyl peaks can be cautiously assigned to the protons on C(M2) and C(M3), with the remaining resonance arising from the methyl group on C(M8).

The signal associated with the unique C–H proton H(7) proved elusive. Although its presence is clearly demonstrated by the splitting of the geminal methyl proton peak as noted, the C–H peak itself is not observable under normal conditions owing to its broad line width arising from unresolved coupling to (1) the adjacent methyl protons (giving a quartet with J = 6 Hz), (2) the $^{11}B(11)$ nucleus (doublet, J = 10–30 Hz), and (3) the proton H(11) (doublet, J = 1–10 Hz). However, with the aid of a triple resonance experiment[18] (broad-band ^{11}B decoupling plus single-frequency homonuclear decoupling), the collapse of the C(M7) doublet was observed by systematically positioning the homonuclear decoupler at frequencies in the expected range of H(7) (δ 3–1.5). When the desired collapse was achieved, the H(7) res-

(14) Closo metallacarboranes of 13 vertices have been structurally characterized,[15a] and the same geometry (corresponding to that shown in Figure 7) has been calculated[15b,c] for $B_{13}H_{13}^{2-}$.

(15) (a) Churchill, M. R.; DeBoer, B. G. *Inorg. Chem.* **1974**, *13*, 1411. (b) Brown, L. D.; Lipscomb, W. N. *Ibid.* **1977**, *16*, 2989. (c) Bicerano, J.; Marynick, D. S.; Lipscomb, W. N. *Ibid.* **1978**, *17*, 3443.

(16) Colquhoun, H. M.; Greenhough, T. J.; Wallbridge, M. G. H. *J. Chem. Soc., Chem. Commun.* **1980**, 192.

(17) Williams, R. E. *Inorg. Chem.* **1971**, *10*, 210.

(18) Miller, V. R.; Grimes, R. N. *Inorg. Chem.* **1977**, *16*, 15.

Table VI. Bond Angles (Deg) in 11-Br$(CH_3)_4C_4B_7H_8$ (III)

C(2)-B(1)-C(3)	52.5 (2)	B(1)-B(6)-B(11)	108.3 (3)
C(3)-B(1)-B(4)	57.4 (2)	C(2)-B(6)-B(5)	107.4 (3)
B(4)-B(1)-B(5)	59.3 (2)	C(2)-B(6)-B(10)	115.6 (3)
B(5)-B(1)-B(6)	60.7 (3)	C(2)-B(6)-B(11)	59.2 (2)
B(6)-B(1)-B(2)	57.2 (2)	B(5)-B(6)-B(10)	60.3 (3)
B(1)-C(2)-B(3)	65.2 (3)	B(5)-B(6)-B(11)	110.3 (3)
B(1)-C(2)-B(6)	63.8 (3)	B(10)-B(6)-B(11)	67.6 (3)
B(1)-C(2)-B(11)	115.7 (3)	C(8)-C(7)-B(11)	102.7 (3)
B(1)-C(2)-C(M2)	116.8 (3)	C(8)-C(7)-C(M7)	111.3 (3)
C(3)-C(2)-B(6)	111.9 (3)	C(8)-C(7)-H(7)	111.9 (3)
C(3)-C(2)-B(11)	104.8 (3)	B(11)-C(7)-C(M7)	113.5 (3)
C(3)-C(2)-C(M2)	120.2 (3)	B(11)-C(7)-H(7)	111.2 (3)
B(6)-C(2)-B(11)	63.6 (3)	C(M7)-C(7)-H(7)	106.3 (3)
B(6)-C(2)-C(M2)	121.6 (3)	C(3)-B(8)-C(4)	60.0 (2)
B(11)-C(2)-C(M2)	121.0 (3)	C(3)-C(8)-C(7)	100.8 (3)
B(1)-C(3)-C(2)	62.3 (2)	C(3)-C(8)-B(9)	108.3 (3)
B(1)-C(3)-B(4)	62.4 (2)	C(3)-C(8)-C(M8)	116.9 (3)
B(1)-C(3)-B(8)	114.5 (3)	B(4)-B(8)-C(7)	136.1 (3)
B(1)-C(3)-C(M3)	118.6 (3)	B(4)-B(8)-B(9)	58.4 (2)
B(2)-C(3)-C(4)	111.6 (3)	B(4)-C(8)-C(M8)	107.8 (3)
C(2)-C(3)-B(8)	108.7 (3)	C(7)-B(8)-B(9)	99.0 (3)
C(2)-C(3)-C(M3)	121.6 (3)	C(7)-C(8)-C(M8)	116.0 (2)
B(4)-C(3)-C(8)	64.2 (2)	B(9)-C(8)-C(M8)	113.7 (2)
B(4)-C(3)-C(M3)	118.4 (3)	B(4)-B(9)-B(5)	60.0 (3)
C(8)-C(3)-C(M3)	118.7 (3)	B(4)-B(9)-C(8)	58.1 (2)
B(1)-B(4)-C(3)	60.1 (2)	B(4)-B(9)-B(10)	105.9 (3)
B(1)-B(4)-B(5)	61.2 (3)	B(5)-B(9)-C(8)	103.8 (3)
B(1)-B(4)-C(8)	106.0 (3)	B(5)-B(9)-B(10)	59.0 (3)
B(1)-B(4)-B(9)	111.4 (3)	C(8)-B(9)-B(10)	102.2 (3)
C(3)-B(4)-B(5)	107.6 (3)	B(10)-B(9)-H(910)	43.0 (2)
C(3)-B(4)-C(8)	55.9 (2)	B(5)-B(10)-B(6)	62.5 (2)
C(3)-B(4)-B(9)	109.1 (3)	B(5)-B(10)-B(9)	59.7 (3)
B(5)-B(4)-C(8)	108.3 (3)	B(5)-B(10)-B(11)	104.7 (3)
B(5)-B(4)-B(9)	60.6 (3)	B(6)-B(10)-B(9)	105.6 (3)
C(8)-B(4)-B(9)	63.5 (2)	B(6)-B(10)-B(11)	57.6 (3)
B(1)-B(5)-B(4)	59.5 (3)	B(9)-B(10)-B(11)	97.8 (3)
B(1)-B(5)-B(6)	58.7 (2)	B(9)-B(10)-H(910)	45.9 (2)
B(1)-B(5)-B(9)	109.0 (3)	C(2)-B(11)-B(6)	57.1 (2)
B(1)-B(5)-B(10)	108.9 (3)	C(2)-B(11)-C(7)	99.1 (3)
B(4)-B(5)-B(6)	101.0 (3)	C(2)-C(11)-B(10)	103.2 (3)
B(4)-B(5)-B(9)	59.3 (3)	C(2)-B(11)-Br	116.6 (2)
B(4)-B(5)-B(10)	107.2 (3)	B(6)-B(11)-C(7)	130.0 (3)
B(6)-B(5)-B(9)	103.3 (3)	B(6)-B(11)-B(10)	54.8 (2)
B(6)-B(5)-B(10)	57.2 (2)	B(6)-B(11)-Br	112.6 (3)
B(9)-B(5)-B(10)	61.4 (3)	C(7)-B(11)-B(10)	98.7 (3)
B(1)-B(6)-C(2)	59.0 (2)	C(7)-B(1)-Br	117.4 (3)
B(1)-B(6)-B(5)	60.5 (3)	B(10)-B(11)-Br	118.6 (3)
B(1)-B(6)-B(10)	113.1 (3)	B(9)-H(910)-B(10)	91.1 (3)

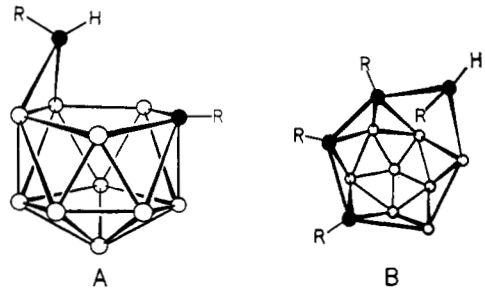

Figure 8. Established structures of other carborane species with bridging carbon atoms: (A) $R_2C_2B_{10}H_{11}^-$ (R = CH_3, C_6H_5);[19a,b] (B) $(CH_3)_4C_4B_8H_9^-$ (characterized as a cobaltocenium derivative).[7] Framework carbon atoms and BH units are depicted as solid and open circules, respectively.

onance was observed (Table II), coincident with a methyl resonance in both C_6D_6 and $CDCl_3$ solution. A similar experiment without ^{11}B irradiation in $CDCl_3$ produced collapse of the methyl doublet only under comparatively high-power (6 mG) decoupling, which is consistent with the expectation that H(7) should resonate over a wide range in the absence of ^{11}B decoupling. The observation of the H(7) peak at δ 2.3 in III (and the corresponding resonance at δ 2.45 in V, an isomer of II discussed below) reinforces these conclusions.

Table VII. Selected Mean Planes in 11-Br$(CH_3)_4C_4B_7H_8$

atom	dev, Å	atom	dev, Å
Plane 1: C(2), C(3), B(4), B(5), B(6) $-0.1892x + 0.1625y - 0.9684z = -2.8690$			
C(2)	−0.0433	B(6)	0.0487
C(3)	0.0154	C(M2)	−0.7625
B(4)	0.0168	C(M3)	−0.6252
B(5)	−0.0376	B(1)	−1.0113
Plane 2: B(9), B(10), H(910) $0.9973x - 0.0369y - 0.0641z = -3.2367$			
B(9)	0.0000	H(910)	0.0000
B(10)	0.0000	B(5)	−0.0774
Plane 3: C(8), B(9), B(10), B(11) $-0.1951x + 0.1642y - 0.9669z = -1.3785$			
C(8)	−0.0209	C(7)	0.8680
B(9)	0.0283	H(910)	0.8776
B(10)	−0.0270	C(M8)	0.4519
B(11)	0.0196	Br	0.6518
Plane 4: C(2), C(3), B(8), B(11) $0.8563x + 0.0770y - 0.5106z = -1.8069$			
C(2)	−0.0204	C(M2)	0.7688
C(3)	0.0213	C(M3)	0.8424
C(8)	−0.0132	C(M8)	0.5182
B(11)	0.0123	C(7)	0.7342
		Br	0.8215
Plane 5: C(2), C(3), B(9), B(10) $0.3509x + 0.1063y - 0.9304z = -3.1173$			
C(2)	0.0026		
C(3)	−0.0026	C(M2)	0.0001
B(9)	0.0022	C(M3)	−0.0044
B(10)	−0.0022	H(910)	0.8110
Plane 6: C(7), C(8), B(11) $-0.9560x + 0.0611y - 0.2868z = 0.6159$			
C(7)	0.0000	Br	−0.2629
C(8)	0.0000	B(4)	0.2066
B(11)	0.0000	B(6)	0.2177
C(M8)	−0.1187	C(M7)	−1.2010
Plane 7: B(1), B(4), B(9), B(10), B(6) $0.7808x + 0.0812y + 0.6195z = -3.5933$			
B(1)	−0.0804	B(6)	0.0897
B(4)	0.0446	H(910)	0.4841
B(9)	0.0061	B(5)	−0.9712
B(10)	−0.0600		

Dihedral Angles between Planes

planes	angle, deg	planes	angle, deg
1,2	97.62	3,4	70.16
1,3	0.36	3,5	31.94
1,4	69.82	3,6	61.71
1,5	31.59	3,7	62.61
1,6	62.06	4,5	38.40
1,7	62.27	4,6	131.88
2,3	97.97	4,7	7.60
2,4	27.89	5,6	93.56
2,5	66.07	5,7	30.80
2,6	159.60	6,7	124.32
2,7	35.38		

The chemical shift of H(7) may be compared with similar protons residing on bridging "methylenic" carbon atoms in other species; thus, in $R_2C_2B_{10}H_{11}^-$ (R = C_6H_5 or CH_3) (Figure 8, A) the shifts are δ 4.77 and 3.55, respectively.[19] In the former species, some deshielding undoubtedly occurs from the geminal phenyl group. In another carborane of this type,[20] $(\eta^5\text{-}C_5H_5)Co(C_5H_4)^+(CH_3)_4C_4B_8H_8^-$ (Figure 8B) the bridging CH proton was

(19) (a) Dunks, G. B.; Wiersema, R. J.; Hawthorne, M. F. *J. Am. Chem. Soc.* **1973**, *95*, 3174. (b) Tolpin, E. I.; Lipscomb, W. N. *Inorg. Chem.* **1973**, *12*, 2257.

(20) Maxwell, W. M.; Grimes, R. N. *Inorg. Chem.* **1979**, *18*, 2174.

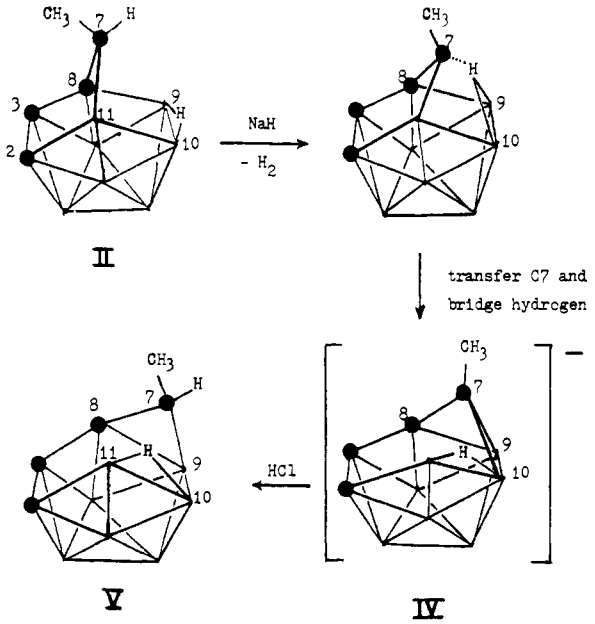

Figure 9. Scheme for conversion of $(CH_3)_4C_4B_7H_9$ (II) to $(CH_3)_4C_4B_7H_8^-$ ion (IV) and $(CH_3)_4C_4B_7H_9$ (V), showing proposed structures of IV, V, and a possible intermediate species. Solid circles indicate framework carbon locations; other vertices are BH.

not observed (though it was crystallographically located[7]) nor was the proton resonance arising from the geminal methyl group split into a doublet; this suggests tautomerization of the proton and/or fluxionality at rates faster than the reciprocal of the coupling constant.

Deprotonation of II and Conversion to a New Isomer. The treatment of $(CH_3)_4C_4B_7H_9$ (II) with excess sodium hydride in THF produced 1 mol equiv of H_2 and generated a $(CH_3)_4C_4B_7H_8^-$ monoanion (IV) as expected. However, reprotonation of this anion with HCl surprisingly failed to regenerate II, giving instead a different isomer (V) which was isolated in 27% yield as a white air-stable solid, mp 140 °C.

The FT NMR spectra of IV and V indicate that both species have substantially different cage structures from II and III, and moreover that IV and V differ from each other. It is evident that deprotonation of II occurs at the bridging CH and not at the B–H–B bridge since in the ^1H NMR spectrum of IV, all four CH_3 resonances are singlets and the B–H–B signal is still present. This result is not unexpected, since deprotonation of $(CH_3)_2C_2B_7H_{11}$ also involves methylenic rather than BHB bridging protons.[11c,21] Also, Williams[22] has suggested a decreasing order of acidity as NH, SH > endo-CH > BHB for arachno carboranes.

Removal of the CH proton in II leaves the bridging carbon coordinately unsaturated, an unstable arrangement which probably induces movement of the bridging CH_3C: unit toward the B–H–B proton as shown in Figure 9. It would then seem reasonable for the bridging hydrogen to move to a new location between B(10) and B(11) as shown, thereby allowing C(7) to bond to B(9) and B(10) and hence achieve incorporation into the cage, as depicted in the suggested stable structure for the anion (IV). The geometry shown for IV is consistent with the ^1H and ^{11}B FT NMR and IR data and represents a significantly altered cage geometry in comparison to the original species, II.

The reprotonation of IV could conceivably follow any of four paths: (1) regeneration of II, (2) reversal of the CH_3 and H positions on C(7) relative to II, (3) protonation of the B(9)–B(10) edge in IV to form a second B–H–B bridge, causing C(7) to move into the framework between C(8) and B(9), or (4) entry of the proton at C(7) to form a -$CH(CH_3)$- bridge between C(8) and B(9), as shown in Figure 9 (V). Possibility 1 is eliminated since II is not observed as a product, and (2) is effectively ruled out

(21) Voet, D.; Lipscomb, W. N. *Inorg. Chem.* **1967**, *6*, 113.
(22) Williams, R. E. *Adv. Inorg. Chem. Radiochem.* **1976**, *18*, 67.

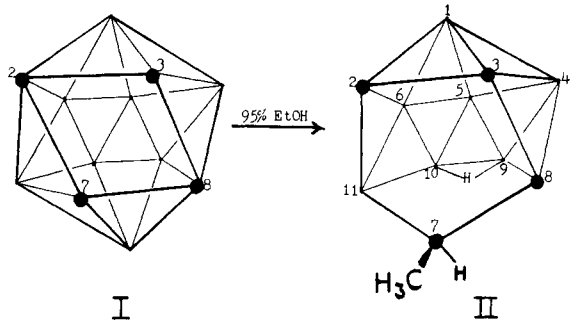

Figure 10. Scheme for formation of $(CH_3)_4C_4B_7H_9$ (II) by degradation of $(CH_3)_4C_4B_8H_8$ (I, isomer B). Solid circles indicate framework carbon atoms.

by the gross differences in the ^{11}B NMR spectra of II and V; mere interchange of the CH_3 and H ligands on C(7) in II would not produce major changes in the boron spectrum. Pathway 3 is eliminated by the appearance of a CH signal at δ 2.45, the observation of an area 1 B–H–B resonance in V, and the fact that one of the methyl signals in the ^1H spectrum is split into a doublet, indicating the presence of a $CH(CH_3)$ bridge. The fourth possibility, however, is supported by the data and is depicted as structure V in Figure 9. We emphasize that the geometries given for IV and V are not established but represent likely arrangements consistent with available evidence.

Conclusions

The degradation of $(CH_3)_4C_4B_8H_8$ (I) to $(CH_3)_4C_4B_7H_9$ (II) is illustrated in Figure 10. From comparison of the established structures of I and II, we envision that the boron removed is B(12), with C(7) accepting a hydrogen atom and moving into the bridging position as shown; the second hydrogen enters the B(9)–B(10) edge to form a B–H–B bridge. The base attack at B(12) indicates that this atom and its counterpart B(1) are the most electrophilic sites in I, consistent with their locations adjacent to two framework carbon atoms. This observation corroborates earlier indications[23] that the attack of $C_2H_5O^-$ on I to form *B,B'*-$(C_2H_5O)_2$-$(CH_3)_4C_4B_8H_6$ occurs at B(1) and B(12);[24] it also follows the pattern set by 1,2-$C_2B_{10}H_{12}$, where the favored sites for base attack are B(3) and B(6), the borons adjacent to two carbon atoms.[11a,b]

The preference for a carbon-bridged structure in II, with placement of a proton on C(7) and movement of that atom out of the cage, is reasonable in that it permits C(7) to achieve a "normal" tetrahedral environment and also allows the remaining framework carbon atoms to adopt low-coordinate vertices on the open face. A similar argument was previously applied[7] to the $(CH_3)_4C_4B_8H_9^-$ ion (Figure 8B).

The fact that only one isomer of II is formed in the degradation implies a single stereospecific process. Similarly, electrophilic bromination of II produces only one detectable isomer (though it is possible others may have formed in low yield), with attack occurring at B(11). This site is perhaps surprising since in the $C_2B_{10}H_{12}$ isomers electrophilic halogenation takes place preferentially at the boron atoms most distant from carbon.[8] Thus, in II one might have expected attack at B(5) or B(10); the fact that it occurs at B(11) indicates that the charge distribution in II is not controlled by simple inductive effects alone.

Finally, the formation of a new isomer of $(CH_3)_4C_4B_7H_9$ (V) on deprotonation of II followed by treatment with HCl implies that V is thermodynamically favored over II (if it is assumed that facile kinetic pathways from the anion IV to both II and V are

(23) Maxwell, W. M.; Wong, K.-S.; Grimes, R. N. *Inorg. Chem.* **1977**, *16*, 3094.
(24) NMR data[23] show that the diethoxy species is symmetrically substituted, but there are four pairs of equivalent boron vertices on $(CH_3)_4C_4B_8H_8$ at which such substitution could occur. However, the fact that the ethoxy group on an analogous cobaltacarborane, $(\eta^5$-$C_5H_5)Co(CH_3)_4C_4B_7H_7$ (isomer I), is located at B(12)[25] is taken as support for 1,12-disubstitution on $(CH_3)_4C_4B_8H_8$ itself.
(25) Pipal, J. R.; Grimes, R. N. *J. Am. Chem. Soc.* **1978**, *100*, 3083.

available). If the proposed structure for V is correct, the preference for V is understandable from the viewpoint that it is less strained than II and closer to icosahedral-fragment geometry. Further development of these ideas will depend on continuing chemical and structural investigations in this area.

Experimental Section

Materials. Tetra-*C*-methyltetracarbadodecaborane(12) [$(CH_3)_4C_4B_8H_8$ (I)] was prepared from the complex $[(CH_3)_2C_2B_4H_4]_2FeH_2$ as described elsewhere.[2] Tetrahydrofuran (THF) was dried over $LiAlH_4$ prior to use. NaH (Alfa, 50% in mineral oil) was washed with pentane prior to use. Thin-layer chromatography (TLC) was conducted on precoated plates of silica gel F-254 (Brinkmann Instruments, Inc.) All solvents were reagent grade.

Instrumentation. ^{11}B (32 MHz) and ^1H (100 MHz) pulse Fourier transform NMR spectra were recorded on a JEOL PS-100P spectrometer interfaced to a JEOL-Texas Instruments EC-100 computer system. Broad-band heternuclear decoupling was employed. The 90-Mz ^1H NMR spectra and some single-frequency homonuclear decoupling experiments were performed on a Varian EM-390 NMR spectrometer. Unit-resolution mass spectra (EI) were obtained on a Hitachi Perkin-Elmer RMU-6E mass spectrometer. High-resolution (CI) mass measurements were conducted on an AEI MS-902 double-focusing instrument equipped with an SRI chemical ionization source. Infrared spectra were recorded on a Beckman IR-8 instrument.

Synthesis of $(CH_3)_4C_4B_7H_9$ (II) from $(CH_3)_4C_4B_8H_8$ (I). In a typical reaction, 219 mg of I (1.07 mmol) was dissolved slowly in 25 mL of 95% ethanol and stirred in air. The progress of the reaction was monitored by spot TLC analysis in hexane (compound I, R_f 0.45) until no I was observed (about 12 h). The ethanol was removed by a rotary evaporator, with some warming of the flask. The residue was extracted with hexane, the solution was filtered through 1-cm silica gel, and the eluant was rotary evaporated nearly to dryness. Residual solvent was removed by blowing dry N_2 over the white solid to give 98.8 mg of $(CH_3)_4C_4B_7H_9$ (II, 0.51 mmol, 48% yield, R_f 0.55 in hexane). The yield of II varied from 40%–60%. The remaining residue in the flask was primarily $B(OH)_3$ (45 mg, 68% yield), identified by IR spectra and its melting point. Similar reactions using lower and higher concentrations of H_2O in ethanol gave lower yields.

The following experiments represent attempts at increasing the yield of the reaction and determining the role of H_2O and solvent in the reaction.

$(CH_3)_4C_4B_8H_8$ in absolute ethanol: 89 mg of I was dissolved in 15 mL of absolute ethanol (dried over molecular sieves) and stirred in vacuo for 8 h. Spot TLC analysis showed only I. Subsequent workup gave 87 mg of I (98% recovery).

$(CH_3)_4C_4B_8H_8$ in methanol: 10 mg of I was dissolved in about 10 mL of methanol (dried over molecular sieves) and stirred in vacuo for 4 h. Spot TLC analysis showed only I. The reaction vessel was then opened to the air and stirred for 12 h, allowing the methanol to absorb water from the air and slowly evaporate. The residue in the flask was purified by TLC to give 4 mg of II (40% yield).

$(CH_3)_4C_4B_8H_8$ in triethylamine: 10 mg of I was dissolved in 10 mL of $(C_2H_5)_3N$ (dried over BaO and P_2O_5) and stirred in vacuo for 4 h. Spot TLC analysis indicated only a trace of I. The $(C_2H_5)_3N$ was removed by a rotary evaporator and the residue was purified by TLC to give about 1 mg of I.

$(CH_3)_4C_4B_8H_8$ in 5% H_2O in THF: 10 mg of I was dissolved in about 10 mL of 5% H_2O in THF and stirred in the air. Spot TLC analysis indicated only I after 15 min. After 6 h, spot TLC showed neither I nor II.

$(CH_3)_4C_4B_7H_9$ in 95% ethanol: 30.1 mg of I was dissolved slowly in 15 mL of 95% ethanol and stirred for 8 h in air. The ethanol was removed at 30–35 °C with the use of a rotary evaporator and the white residue was purified by TLC to give 22.8 mg II (75% recovery).

Direct Synthesis of II from the $(CH_3)_2C_2B_4H_5^-$ Ion.[12] A THF solution of $Na^+[(CH_3)_2C_2B_4H_5]^-$, prepared from 5.12 mmol of $(CH_3)_2C_2B_4H_6$ and 5.85 mmol of NaH, was filtered under vacuum onto anhydrous $FeCl_2$ at −196 °C. *This mixture was allowed to come to room temperature*, in contrast to previous preparations[2] of $[(CH_3)_2C_2B_4H_4]_2FeH_2$ in which the temperature was held below −30 °C. After 1 h the THF was removed under vacuum and CH_2Cl_2 was added. The solution was stirred in air for 1 h, and the products were separated and purified via column and thin-layer chromatography. In addition to previously reported compounds,[2] II was isolated in low yield. Mass measurement: calcd for $^{12}C_8{}^{11}B_7{}^1H_{20}{}^+$ (M + 1), 193.2217; found, 193.2223. The IR and FT NMR spectra were identical with those in Tables I–III.

Bromination of $(CH_3)_4C_4B_7H_9$. Under a nitrogen atmosphere, a 25-mL three-neck round-bottom flask was charged with 41.6 mg of $AlCl_3$ (0.313 mmol, 1.3 equiv, freshly sublimed in vacuo) and a magnetic stirbar. One port was affixed with a N_2 inlet to maintain an overpressure of N_2, and a second port was affixed with a tip-in side arm containing 46.0 mg of II (0.239 mmol, 1.0 equiv) dissolved in 5 mL of CS_2 (dried over $CaCl_2$ and over P_2O_5). A 10.0-mL aliquot (0.29 mmol of Br_2) of a solution of 116.5 mg of Br_2 in 25.0 mL of CS_2 was put in a pressure-equalizing dropping funnel under a N_2 flow at the third port. The Br_2 solution was added to the $AlCl_3$, with no apparent reaction, and the carborane was tipped into the reaction vessel. After 1 h of stirring at room temperature with no apparent reaction, the funnel was replaced by a reflux condenser and the solution was slowly refluxed for 5 h, under N_2, giving a brownish red solution and some light and dark precipitates. The reactor was then exposed to the air, the CS_2 removed with the use of a rotary evaporator, and the residue was dissolved in CH_2Cl_2 and filtered through 1-cm silica gel and a glass frit. The CH_2Cl_2 solution was rotary evaporated to give a cream colored residue. TLC in 30% CH_2Cl_2/hexane (R_f 0.6) gave 32.5 mg of 11-$Br(CH_3)_4C_4B_7H_8$ (III, 0.119 mmol, 50% yield).

Deprotonation of II. Synthesis of $(CH_3)_4C_4B_7H_9$ (V). A 37-mg sample of II (0.19 mmol), 23 mg of NaH (1.0 mmol), and a stirbar were placed in a tip-in side-arm flask which was evacuated, and 15 mL of dry THF was added by distillation in vacuo. The flask was slowly warmed to 23 °C, with vigorous bubbling (H_2 evolution) occuring below 0 °C. After 30 min of stirring (H_2 evolution ceased), the solution was frozen and H_2 pumped away (not measured, but see below), and after being warmed to 23 °C, the solution was filtered in vacuo into a lower flask containing a stirbar. (The side-arm flask containing residual NaH was removed under N_2 atmosphere, and the port was plugged with a stopper.) The solution was frozen, and 2.8 mmol HCl was transferred as a gas onto the frozen solution. The solution was then warmed to 23 °C and stirred for 3 h. The system was covered with N_2 and exposed to the air, and the THF removed by a rotary evaporator. The white residue was purified by TLC in hexanes to give $(CH_3)_4C_4B_7H_9$ (V, 10 mg, 27% yield, R_f 0.45) and a trace of an unidentified white compound at R_f 0.60. The mass spectrum of V is closely similar to that of II, except that significant intensity is observed in the parent peaks at m/e 193 and 194, indicating that loss of two H from V is less facile than from II (vide supra).

In a similar experiment, 60 mg of II (0.31 mmol) was deprotonated with 37 mg of NaH (1.5 mmol). H_2 evolved was measured to be 0.33 mmol (106% of theoretical amount). The salt was filtered into an empty flask, and the THF was removed in vacuo. In a drybox under an atmosphere of N_2, the salt was dissolved in CD_3CN and filtered into an NMR tube (capped and wrapped with parafilm) for NMR analysis. Subsequent exposure to air indicated slow decomposition of the salt to an insoluble (in CD_3CN) white solid. Before decomposition was complete, the CD_3CN was removed by a stream of N_2 and the white residue was dissolved in 5 mL of 95% ethanol and 1 mL of 0.3 M aqueous HCl. After 1 h of stirring in air, the EtOH/H_2O was removed by rotary evaporator. TLC analysis showed only a trace of unidentified material at R_f 0.35 in hexane.

X-ray Structure Determination on 11-$Br(CH_3)_4C_4B_7H_8$ (III). Single crystals of III were grown by slow evaporation from $CDCl_3$ at 10 °C. One crystal was mounted on a glass fiber in an arbitrary orientation and examined by preliminary precession photographs which indicated acceptable crystal quality. Crystal data were as follows: $BrC_8B_7H_{20}$; mol wt 271.84; space group $P\bar{1}$; $Z = 2$; $a = 7.764$ (3), $b = 8.352$ (5), $c = 12.317$ (6) Å; $\alpha = 94.53$ (5), $\beta = 95.41$ (5), $\gamma = 120.51$ (5)°; $V = 678$ Å^3; μ(Mo Kα) = 31.8 cm^{-1}; ρ(calcd) = 1.34 g cm^{-3}. Crystal dimensions (mm from centroid): (100) 0.35, (010) 0.23, (0$\bar{1}$0) 0.23, (1$\bar{1}$0) 0.24, ($\bar{1}$10) 0.24, (001) 0.055, (00$\bar{1}$) 0.055.

For this crystal the Enraf-Nonius program SEARCH was used to obtain 25 accurately centered reflections which were then used in the program INDEX to obtain an orientation matrix for data collection and to provide approximate cell dimensions. Refined cell dimensions and their estimated standard deviations were obtained from 28 accurately centered reflections. The mosaicity of the crystal was examined by the ω scan technique and judged to be satisfactory. The space group was chosen on the basis of systematic absences and chemical and spectroscopic information. Successful solution and refinement of the structure confirmed the choice of space group.

Collection and Reduction of the Data. Diffraction data were collected at 295 K on an Enraf-Nonius four-circle CAD-4 diffractometer controlled by a PDP8/M computer with use of Mo Kα radiation from a highly oriented graphite crystal monochrometer. The θ–2θ scan technique was used to record the intensities of all reflections for which $1.4° < 2\theta < 48°$. Scan widths were calculated from the formula SW = (A + B tan θ), where A is estimated from the mosaicity of the crystal and B compensates for the increase in the width of the peak due to Kα_1–Kα_2 splitting. The values of A and B were 0.60 and 0.35, respectively. The calculated scan angle was extended at each side by 25% for background determination (BG1 and BG2). The net count (NC) was then calculated

as NC = TOT - 2(BG1 + BG2), where TOT is the estimated peak intensity.

The intensities of four standard reflections, at 100-reflection intervals, showed no greater fluctuations during the data collection than those expected from Poisson statistics. The raw intensity data were corrected for Lorentz-polarization effects and then for absorption (minimum transmission factor 0.46, maximum 0.78), resulting in 2038 reflections of which 1404 had $F_o^2 > 3\sigma(F_o^2)$, where (F_o^2) was estimated from counting statistics ($p = 0.03$).[26] Only these latter data were used in the final refinement of the structural parameters.

Solution and Refinement of the Structure. Full-matrix least-squares refinement was based on F, and the function minimized was $w(|F_o| - |F_c|)^2$. The weights w were taken as $[2F_o/\sigma(F_o^2)]^2$, where $|F_o|$ and $|F_c|$ are the observed and calculated structure factor amplitudes. The atomic scattering factors for nonhydrogen atoms were taken from Cromer and Waber[27] and those for hydrogen from Stewart et al.[28] The effects of anomolous dispersion for all nonhydrogen atoms were included in F with use of the values of Cromer and Ibers[29] for $\Delta f'$ and $\Delta f''$.

The position of the Br atom was determined from a three-dimensional Patterson function calculated from all the intensity data. The intensity data were phased sufficiently well by these positional coordinates that difference Fourier syntheses revealed most of the nonhydrogen atoms, the remaining nonhydrogen atoms being inserted in calculated positions. Most of the cage hydrogen atoms were found from a Fourier difference map after introducing anisotropic thermal parameters for all nonhydrogen atoms. At least one hydrogen on each methyl group was found; the remaining hydrogen positions were calculated and inserted. The hydrogen atoms were included in the refinement for three cycles and thereafter held fixed. A final Fourier difference map was featureless. The error in an observation of unit weight was 1.96, and the largest parameter shift in the last cycle of refinement was 0.25 times the estimated standard deviation.

The model converged with $R = 0.057$ and $R_w = 0.063$, where $R = \sum||F_o| - |F_c||/\sum|F_o|$ and $R_w = [\sum w(|F_o| - |F_c|)^2/\sum w|F_o|^2]^{1/2}$. Tables of observed and calculated structure factors are available (see paragraph at end of paper on supplementary material). The computing system and programs are described elsewhere [30]

Acknowledgment. This work was supported by the Office of Naval Research and the National Science Foundation, Grant No. CHE 79-09948. We are grateful to Mr. William Hutton for assistance in recording the NMR spectra and to Professor Ekk Sinn for assistance in the X-ray structure determination.

Supplementary Material Available: Listing of observed and calculated structure factors (6 pages). Ordering information is given on any current masthead page.

(26) Corfield, P. W. R.; Doedens, R. J.; Ibers, J. A. *Inorg. Chem.* **1967**, *6*, 197.
(27) Cromer, D. T.; Waber, J. T. "International Tables for X-ray Crystallography"; Kynoch Press: Birmingham, England, 1974; Vol. IV.
(28) Stewart, R. F.; Davidson, E. R.; Simpson, W. T. *J. Chem. Phys.* **1965**, *42*, 3175.
(29) Cromer, D. T.; Ibers, J. A. Reference 27.
(30) Freyberg, D. P.; Mockler, G. M.; Sinn, E. *J. Chem. Soc., Dalton Trans.* **1976**, 447.

Excited States of Mixed-Ligand Chelates of Ruthenium(II). Quantum Yield and Decay Time Measurements[1a]

W. H. Elfring, Jr., and G. A. Crosby*[1b]

Contribution from the Department of Chemistry, Washington State University, Pullman, Washington 99164. *Received January 10, 1980. Revised Manuscript Received January 5, 1981*

Abstract: The photoluminescence of a series of $[Ru(II)(bpy)_m(N\text{-}N)_n]^{2+}$ cations [$m = 3 - n$; $n = 0, 1, 2, 3$; bpy = 2,2'-bipyridine; N-N = 1,10-phenanthroline (phen) or substituted phen or substituted bpy] was investigated. All compounds displayed a prominent visible luminescence, a single ~1.3 kK vibration progression, and an ~5 μs decay time at 77 K that increased monotonically as the temperature was lowered. Quantum yields at 77 K ranged between 0.35 and 0.58. The data were analyzed in terms of a charge-transfer-to-ligand excited manifold of three levels.

Ruthenium(II) complexes containing π-conjugated ligands have become the focus of a variety of photochemical,[2] electrochemical,[3] and spectroscopic investigations.[4,5] The fascination is elicited by the occurrence of charge-transfer-to-ligand (CTTL) excited states that endow the complexes with rich visible absorption spectra and, when the ligand field strengths are sufficiently high, with a visible luminescence that can be stimulated in a variety of ways. Moreover, these complexes display luminescence in fluid solution. Thus, they possess important measurable physical parameters that can add insight to mechanistic considerations of photophysical and photochemical processes.[6] In addition to the lively fundamental interest generated by these materials in the field of excited state chemistry, a further impulse to investigate them is occasioned by the circumstance that they not only absorb visible light but are theoretically capable of splitting water into its elements by the utilization of solar energy.[7]

Our interest in Ru(II) complexes has evolved from the intention to provide physical and mathematical models of the excited states of transition metal complexes based on photophysical measurements. For these studies, extending over a decade, Ru(II) complexes with 2,2'-bipyridine (bpy) and 1,10-phenanthroline (phen) ligands have played a pivotal role because the $(4d)^6$ strong-field configuration and the low-lying ligand π* orbitals provide the proper disposition of energy levels such that intense emission occurs from excited states that are clearly charge transfer to ligand in nature. This luminescence has provided the tool to probe the innate properties of CTTL states and has led to a coherent description of them that can, we conjecture, be applied with some confidence to CTTL states exhibited by complexes of other elements and other electronic configurations.[4,5]

Recently, we have completed our investigations of the analogous complexes of Os(II) and have given a description of the CTTL

(1) (a) Research sponsored by the Air Force Office of Scientific Research, Air Force Systems Command, USAF, under Grant No. AFOSR-76-2932; (b) U.S. Senior Scientist (Humboldt Awardee), Universität Hohenheim, West Germany, 1978-1979.
(2) Balzani, V.; Moggi, L.; Manfrin, M. F.; Bolletta, F.; Laurence, G. S. *Coord. Chem. Rev.* **1975**, *15*, 321. Meyer, T. J. *Israel J. Chem.* **1976/77**, *15*, 200.
(3) Tokel-Takvoryan, N. E.; Hemingway, R. E.; Bard, A. J. *J. Am. Chem. Soc.* **1973**, *95*, 6582. Laser, D.; Bard, A. J. *J. Electrochem. Soc.* **1975**, *122*, 632. Gleria, M.; Memming, R. *Z. Phys. Chem. (Wiesbaden)* **1975**, *98*, 303.
(4) Hager, G. D.; Crosby, G. A. *J. Am. Chem. Soc.* **1975**, *97*, 7031.
(5) Hager, G. D.; Watts, R. J.; Crosby, G. A. *J. Am. Chem. Soc.* **1975**, *97*, 7037.
(6) Demas, J. N.; Adamson, A. W. *J. Am. Chem. Soc.* **1971**, *93*, 1800.
(7) Meyer, T. J. *Acc. Chem. Res.* **1978**, *11*, 94.

0002-7863/81/1503-2683$01.25/0